

Feedback between deglaciation and volcanic emissions of CO₂

Peter Huybers and Charles Langmuir

Department of Earth and Planetary Sciences, Harvard University
Cambridge, MA 02138, USA. e-mail: phuybers@fas.harvard.edu

A global reconstruction of subaerial volcanic activity over the last 40 Kyr shows a pervasive high-latitude increase in volcanism between 12 Ka and 7 Ka that more than doubles global volcanic activity. This increase can be understood as a consequence of melt generated in response to deglacial decompression. We estimate that increased volcanism during this 5 Ka period emitted an additional 1000 to 5000 Gt of CO₂ into the atmosphere. Such a flux is consistent in timing and magnitude with ice core observations of a 40 ppm increase in atmospheric CO₂ concentration during the second half of the last deglaciation. Anomalous volcanic emissions also persist later into the Holocene, and it appears that elevated volcanic activity helps maintain high levels of CO₂ during interglacials.

Ice volume and atmospheric CO₂ concentrations vary in near lock-step with one another over the course of the late Pleistocene glacial/inter-glacial cycles. The ocean is an obvious candidate for control of glacial time scale variations in atmospheric CO₂ (*I*), even if the exact mechanisms are uncertain, because this large carbon reservoir exchanges with the atmosphere over millennial and shorter time scales. Here we argue that the vast carbon reservoir associated with the solid Earth also influences the ocean-atmosphere system at millennial timescales and, in particular, that deglaciation induces volcanism and thereby increases atmospheric CO₂ concentrations. In this view, volcanism forges a link between glacial variability and atmospheric CO₂ concentrations.

Deglaciation and increased volcanism

Volcanism influences climate at time scales ranging from annual (2) to tectonic (3). Evidence has also accumulated for the converse, that climate influences volcanism (4). Earth tides (5–8), atmospheric pressure and temperature (9), and water storage (10, 11) all appear to influence the timing of certain volcanic eruptions. If such subtle changes in environment can influence eruptions, it is no surprise for the massive changes environment associated with deglaciation to also affect volcanism (12–19). Indeed, deglaciation coincides with increased volcanism in Iceland (14, 17, 20, 21), France and Germany (22), eastern California (19, 23), the Pacific Northwest (24), and Chile (4, 25, 26). This confluence of evidence suggests that deglaciation promotes a widespread increase in volcanism, perhaps of sufficient scale to feed back upon global climate.

But are these indications of increased deglacial volcanism more than outliers picked from a background of volcanic variability? To test the global extent and magnitude of increased volcanism during the last deglaciation we combine a dataset of volcanic eruptions over the last 40Ky (27) with a much more complete dataset covering only the Holocene (28, 29), removing redundant events. We also remove small events (having a volcanic explosive index less than two) and events whose ages which are not bracketed between certain dates, leaving a total of 5352 volcanic events during the last 40,000 years. We exclude small events because these are less likely to be consistently identified in the past (28, 29). Nonetheless, there exists a bias against older observations — 80% of dated eruptions are less than 1000 years old (Fig. 1) — which needs to be considered carefully in the temporal and spatial evaluation of the data.

The age of each volcanic event is represented using a probability distribution (30) and the location is represented using global maps of volcanic activity. Activity is calculated as a function of longitude and latitude using a weighted average, $A(\phi, \theta) = \sum_{i=1}^N P_{i,j} \lambda_i$ where $P_{i,j}$ is the probability that event i occurred during interval j . The weighting term, $\lambda_i = s/(s + r_i)^2$, depends on the distance, r_i , between each point, (ϕ, θ) , and each volcanic event, i . The smoothing length scale, s , is set to 500 km. We select three distinct intervals — the glacial (40 Ka to 20 Ka), the deglacial (17 Ka to 7 Ka), and the late Holocene (5 Ka to the present) — and explore changes in the dis-

tribution of volcanism by computing the ratio of deglacial activity first to the glacial and then to the late Holocene activity (Figs. 2a,b). Both of these activity ratio maps indicate that the relative proportion of volcanic activity shifted toward the Southern Andes, Kamchatka, the Aleutian Arc, and the Cascades and Cordillera regions during the last deglaciation, a list which comprises all the major volcanic regions that appear to have experienced substantial unloading of ice during the last deglaciation (21, 31–35). Importantly, both maps show consistent patterns even though the the deglacial/glacial activity is biased towards high values and deglacial/late-Holocene activity ratios are biased low by the diminishing observations back in time. This consistency in the face of opposite biases indicates that the increase in deglacial volcanic activity observed at high latitudes is not an artifact of observational bias.

To better quantify the relationship between volcanism and deglaciation it is useful to develop a globally mapped proxy to indicate which regions undergo deglaciation. We estimate such a deglaciation proxy using the modern ice mass balance obtained from temperature and precipitation reanalysis (36, 37). Reassuringly, regions predicted to have the greatest modern mass balance are glaciated today (38) (Fig. 2c) and were more glaciated in the past (31, 32). To compare the deglacial activity ratios to the deglaciation proxy, we first normalize each of the two activity ratio maps to unit standard deviation (to remove the effects of observational bias) and then average them together. Activity ratios increase markedly when the ice mass balance is greater than -6 m/yr (Fig. 3). For example, activity ratios along the Western Pacific Rim increase by more than a factor of five between the tropics and the more glacially-prone northern regions. Along with earlier regional studies, our global analysis of volcanic events supports the hypothesis of a deglacial influence on volcanism.

Temporal variability of global volcanic activity

The foregoing analysis suggests that volcanic events are divisible into unglaciated regions, presumed to have a steady activity rate, and glaciated regions, presumed sensitive to ice unloading. It is then possible to examine the temporal change in volcanism and account for the reporting bias by normalizing the data from glaciated regions to that from unglaciated regions. We approximate the

true frequency of eruptions in unglaciated regions as a constant, u_o , and relate it to the observed frequency, u' , using an observational bias term, $u'_t = u_o b_t$. The bias term, b_t , is expected to decrease with time as a power-law process (28). For glaciated regions we have $g'_t = g_t b_t$, where the true frequency, g_t , is time dependent. Assuming that the sampling bias is consistent between both groups (39) allows us to use the frequency of unglaciated eruptions as a control by which to estimate the glaciated frequency, $g_t = u_o g'_t / u'_t$. Global volcanic frequency is then $v_t = u_o (1 + g'_t / u'_t)$, which we present as fractional deviations from the present, $v_t / v_o = (1 + g'_t / u'_t) / (1 + g_o / u_o)$.

The mass balance estimates provide a measure to divide the volcanic events into glaciated and unglaciated groups. A threshold of -9 m/yr gives an equal frequency of events between the glaciated and unglaciated groups during the last 2 Kyr, though a threshold of -6 m/yr also seems plausible based on where activity shifts toward higher values (Fig. 3). Either threshold indicates that the ratio of glaciated to unglaciated eruption frequencies, g'_t / u'_t , is lowest during the last glacial, built rapidly near ~ 12 Ka, peaks at 7 Ka, and then subsides back toward glacial levels in the recent past (Fig. 4b). The -6 m/yr threshold indicates that global activity was double that of today between 12 Ka and 7 Ka, whereas -9 m/yr indicates that global activity increased by a factor of five, and we expect that the actual value lies between these bounds. Regardless of which threshold is used, the increase in volcanic activity above modern values is statistically highly significant ($p < 0.01$) (40).

Our estimate of the time-history of global volcanism is consistent with an independent, more regional estimate from Greenland (41), which indicates that the interval between 15 Ka to 8 Ka has the greatest frequency of volcanic events and that the interval between 13 Ka and 7 Ka has the largest eruptions. That an uptick in volcanic activity occurs at 12 Ka, as opposed to the beginning of the deglaciation at 18 Ka, can be understood in that deglaciation in Northern volcanic regions — including Alaska (33), the Cordillera (34), and Iceland (21) — appears most pronounced near 12 Ka. The deglaciation of southern South America appears spread out over a longer interval, initiating near 17 Ka and proceeding in a series of steps toward almost complete deglaciation by 11 Ka (35). A further possibility is for there to be poor preservations of tephra from eruptions early in the deglaciation because of emplacement onto ice that subsequently melted away. There also

exists the possibility that rising sea level would suppress volcanic activity on islands (42–44), but recalculation excluding all island volcanoes yields similar results.

Physical Mechanisms

Glacial unloading can directly influence volcanic activity by decreasing mantle pressure, which increases melt production and the potential for eruption (17). Unloading 1 km of ice decreases the underlying pressure by 10 MPa and would melt 0.1% of a melt region, or produce 100 m of melt in a region 100 km thick. Mountain glaciers and small ice caps are estimated to have decreased in volume from 1.9 million km³ during the Last Glacial Maximum to a volume of 0.12 million km³ today (31). If only a tenth of the glacier loss influences magmatic production (consistent with unloading 200 m thick ice from a 60 km swath along 15,000 km of convergent margin) one anticipates 18,000 km³ of melt production. This is akin to doubling global subaerial volcanism for 5000 years. If a quarter of the glacier melt is involved, melt production is consistent with a five-fold increase in subaerial volcanism for 5000 years. Thus, the upper and lower bounds on volcanic activity from the volcanic eruption data are broadly consistent with the magmatic production expected from unloading of mountain glaciers and small ice caps. A more rigorous analysis of volcanism in Iceland found that the deglaciation of a 2 km thick ice cap was responsible for 3100 km³ of erupted material (17,21), consistent with the timing and extent of dated lava flows and in keeping with our global estimate. Following the same logic, we expect the deglacial rise in sea-level to decrease submarine volcanism, a point to which we return later.

Glacial loading and unloading could also serve to pace eruptions. The eruptability of a particular volcano can be viewed as a balance between the forces generated by melt and gas production within the volcano edifice and the confining pressure and integrity of the surrounding rocks. Removing ice reduces the confining pressure and could trigger volcanoes near the threshold of eruptability. Volcanic systems with recharge time scales similar to that of the glacial cycles may become phase locked with the climate forcing (45). In this scenario, even a weak climate effect could cause synchronization of volcanic eruptions with deglaciation. Volcanic systems with longer time scales tend to be larger, so that systems that become phase-locked with glacial cycles are liable to be

among the largest. These effects could lead to an even greater volume of eruptions than would result from the pressure-melting effects discussed above. Furthermore, far field effects, such as from the unloading of the continents and the rising sea level, may encourage volcanism by opening passageways or altering the pressure in magmatic chambers (15, 18, 44).

It is also worth noting that the co-location of glaciation and volcanoes is no accident. The elevation and orographic influences on precipitation inherent to volcanic regions will promote glaciation. In addition, the current plate configuration puts many volcanoes at high latitudes and on the western flank of the Americas, thus giving mountains well-situated to capture precipitation from the moisture-laden westerlies coming off the Pacific and to retain it as ice. The Sea of Okhotsk also contributes to precipitation in Kamchatka. Thus we should expect a close correspondence between the locations of mountain glaciers and volcanoes, particularly for our current plate configuration.

Implications for the carbon cycle

The data demonstrate a relationship between deglaciation and greater volcanic activity. We hypothesize that elevated volcanism during deglaciations contributes to the rise in atmospheric CO₂ during deglaciation and sets up a positive feedback wherein increased greenhouse gases promote further deglaciation and volcanic activity. Conversely, waning volcanic activity during the Holocene would contribute to cooling and reglaciation, thus tending to suppress volcanic activity and promote the onset of an ice age. This hypothesis depends on the amount of CO₂ emitted from volcanoes, as well as the amount which remains airborne. In principle, such a calculation depends upon nearly all aspects of the climate system, including parts of the solid earth. We are nonetheless able to make order-of-magnitude estimates through scaling modern CO₂ emissions by our estimates of past volcanic activity. We then represent the accumulation of CO₂ in the atmosphere and its equilibration with the ocean using a simple, two box model.

There are various approaches to quantifying modern CO₂ fluxes from convergent margins and ocean ridges. The first is to estimate CO₂ flux from global magma production rates. Long term estimates for crustal production at convergent margins are estimated to be 20 to 40 km³ per km of arc length per Ma (46), but this estimate has been criticized as being too low by a factor of two (47),

and both of these estimates are minima with respect to magma additions because they are the net of production after losses due to erosion. A value of $80 \text{ km}^3/\text{km}/\text{Ma}$ and a 35,000 km total arc length gives a magma production rate of more than $3 \text{ km}^3/\text{yr}$, in accord with other estimates (47–49). The long term average CO_2 flux can be obtained by multiplying magma production rates by the primary CO_2 contents of arc magmas, but primary CO_2 cannot be determined directly because it is almost entirely degassed prior to erupting (50). We estimate the concentration of carbon in the mantle by multiplying an average CO_2/Nb ratio of ~ 500 (51, 52) by an average Nb content of ~ 3 ppm in arc basalts, yielding 0.15% CO_2 in the mantle, in agreement with estimates based on modeling the ^3He flux from the mantle (53, 54). Because carbon isotope data and $\text{CO}_2/^3\text{He}$ ratios both indicate that the mantle contributes only 10% to 20% of the total CO_2 at arc volcanoes (53, 54), we arrive at a total estimate of 0.65% to 1.5% CO_2 in primary arc magmas. 1% CO_2 and $3 \text{ km}^3/\text{yr}$ of magma production leads to a global emission rate of 0.1 Gt/yr (assuming a density of $3 \text{ Gt}/\text{km}^3$). It is harder to parse emissions from non-convergent margin subaerial volcanoes, but they likely add another 0.05 Gt/yr (53, 55). Note that no distinction is made between CO_2 contributions from intruded and extruded magma because we expect the CO_2 to outgas in either case (56, 57).

An alternative estimate of CO_2 emissions relies on data from currently active volcanoes. Williams et al. (58) used global estimates of SO_2 combined with CO_2/SO_2 ratios to estimate current emissions of 0.07 ± 0.05 Gt of CO_2 per year. The implied lower bound, however, seems inconsistent with the measurement that Mt. Etna alone emits 0.04 Gt/year. Inclusion of data from Popocatepetl Volcano (59), which began erupting after the Williams et al. study, would have increased the estimate by 15%. Other authors have used $\text{CO}_2/^3\text{He}$ ratios to estimate global carbon flux from arc volcanoes (53, 55, 60–62), with most estimates near 0.1 Gt/year. A recent simulation of arc volcanism combined with observational studies (63) suggests that the range of emissions found in these other studies are plausible, but the upper end of the range (~ 0.14 Gt CO_2/yr) is most likely. We thus estimate modern subaerial volcanic emissions to be between 0.1 to 0.15 Gt CO_2/year .

Assuming that past changes in volcanic activity are proportional to changes in volcanic CO_2 emissions, the time history of CO_2 fluxes can be estimated by multiplying current volcanic emis-

sions by the ratio between past and present volcanic activity. Lower and upper bounds on CO₂ emissions come from selecting, respectively, mass-balance thresholds of -6 m/yr and -9 m/yr and modern fluxes of 0.1 and 0.15 Gt of CO₂ per year. This leads to 1000 to 5000 Gt of CO₂ emitted above a baseline scenario of current emissions during the last deglaciation.

It is also necessary to account the rise in sea level following from the unloading of ice from the continents, which will tend to decrease ridge volcanism. Because water is roughly a third the density of the mantle, the 135 m deglacial rise in sea level is equivalent to suppressing 45 m of mantle ascent beneath an ocean ridge. Given an average mantle upwelling rate of ~ 3 cm/yr, this is equivalent to suppressing ~ 1500 yrs of melt at ridges. Measurements of CO₂/³He and CO₂/Nb ratios from ridge system indicate that total emissions are ~ 0.1 Gt/yr (51–53). 1500 yrs of lost emissions then equates to ~ 150 Gt CO₂, or an order of magnitude less than the estimated increase in arc CO₂ emissions. Ridges have a minor influence on carbon emissions because they are depleted in CO₂ by a factor of 5 to 10 relative to arc volcanism (51–54), and the greater rates of magma production at ridges means that variations in loading cause smaller fractional changes in magma production and CO₂ emissions. Thus the suppression of ridge volcanism by rising sea-level has little consequence for ocean-atmosphere carbon values.

While volcanic emissions and silicate weathering of CO₂ are largely in balance with one another at million year time scales (3), we expect the increased flux of CO₂ from subaerial volcanism during deglaciation to transiently increase the concentration of atmospheric CO₂. A simple two-box model, similar to that of (64), is used to estimate the time variable volcanic influence upon atmospheric CO₂,

$$\begin{aligned} da/dt &= -F_t + V_t - W_o, \\ db/dt &= F_t. \end{aligned} \tag{1}$$

Here a and b are the amounts of inorganic carbon in the atmosphere and ocean, measured in Gt of CO₂. The atmosphere-ocean flux is $F = (a' - b'(1 - q))/\tau$, where the primes indicate anomalies away from equilibrium. q represent the fraction of volcanic carbon remaining in the atmosphere once the atmosphere comes into equilibrium with the ocean and is taken to be between 10% and

15% (65,66). Estimates of τ range from ~ 300 years (65) to ~ 1800 years (66), depending on which model is used and which feedbacks are included. Even longer ocean equilibration time scales are possible (67), and we assign wide bounds on τ of 300 yrs to 2000 yrs. V is the volcanic flux of carbon into the atmosphere. We assume that at 100 Ky time scales the volcanic flux is balanced by the carbon sink associated with silicate weathering, W , and that the average CO_2 emissions between 40 and 20 Ka equal the unmonitored rates between 100 Ka and 40 Ka. Note that while this model is simplistic, it is able to reproduce the major features in the time history of atmospheric CO_2 found in more complete atmosphere-ocean carbon models (64, 65).

To explore the range of possible atmospheric CO_2 scenarios consistent with our estimates, we perform an ensemble of 10,000 model runs using parameters drawn from a uniform distribution between the upper and lower bounds discussed previously. The box model is initialized at 40 Ka with the atmosphere and ocean in equilibrium. We compare the time history of atmospheric CO_2 expressed in the ensemble of model runs against observation from the Dome C (68) and Taylor Dome (69, 70) ice cores in four intervals (Fig. 4d,e). (1.) During the glacial, between 40 Ka and 18 Ka, model results indicate atmospheric CO_2 decreases by 10 ppm (5 to 20 ppm, 90% c.i.), marginally consistent with the observed 20 ppm decrease. This suggests that the trend toward lower atmospheric CO_2 levels during glaciation is, at least in part, attributable to excess weathering relative to volcanic emissions. (2.) The first half of the deglaciation (18 and 13 Ka) contains a modest ~ 10 ppm (5 to 40 ppm, 90% c.i.) volcanogenic CO_2 increase, whereas observations show a 50 ppm rise. As is well appreciated, factors independent of volcanism exercise important controls on glacial-interglacial variations in CO_2 (1, 71), a point highlighted by the minimal volcanic CO_2 emissions during this interval. (3.) The second half of the deglaciation (13 Ka to 7 Ka), however, contains a 40 ppm (15 to 70 ppm, 90% c.i.) increase in volcanogenic CO_2 which is consistent with the observed increase in atmospheric CO_2 , particularly with respect to the sharp uptick starting at 12 Ka (Fig. 4). (4.) In the late Holocene, after 7 Ka, volcanic CO_2 contributions wane owing to lower volcanic activity and on-going equilibration with the oceans, while observations instead indicate rising CO_2 levels during this interval. It appears that this divergence between the expected

volcanogenic CO₂ and observations is peculiar to the Holocene, a point to which we return.

Tests of the Volcanic Hypothesis

To test our hypothesis of enhanced volcanic emissions of CO₂ during deglaciation, we first consider the implications of a 1000 to 5000 Gt CO₂ release from volcanoes for the ocean carbonate system. The vast majority of CO₂ emitted by volcanoes eventually enters the oceans, increasing ocean acidity and, absent other effects, leading to a shoaling of the carbonate saturation horizon. If we assume that volcanoes injected ~3000 Gt CO₂ into the ocean, and also account for a 4°C ocean warming (72) and 100 ppm increase in atmospheric CO₂ concentration coming out of the last glacial, we expect the carbonate compensation depth to shoal by one to two km. Such a shoaling is consistent with observations of carbonate dissolution in the Pacific (73,74) but not the Atlantic (74). However, this carbon emission scenario neglects the biospheric uptake of ~1500 Gt CO₂ indicated by the ~0.3 per mil increase in ocean $\delta^{13}\text{C}$ between the glacial and Holocene (75). Furthermore, an additional ~500 Gt CO₂ of biological uptake is needed to compensate for volcanic emission of carbon having an isotopic ratio of -3.8 ± 1.2 per mil (61, 76, 77). When we account for this offsetting biological uptake, the expected changes in carbonate saturation horizon is no more than a few hundred meters. A definitive calculation of how volcanic emissions influence carbonate chemistry is precluded by uncertainties in other key components of the system, e.g. coral reef building (78), but we can conclude that the observed changes in ocean carbonates do not conflict with a sizable volcanogenic CO₂ flux.

It is also possible to test the glacio-volcano-CO₂ hypothesis using proxy data from previous interglacials. Our findings indicate that deglaciation triggers greater volcanic emissions of CO₂ and that these anomalous emissions persist into interglacials. Interglacial trends in CO₂ should thus be more positive following larger deglaciations. The combined atmospheric CO₂ records from Vostok (79) and EPICA Dome C (80) permit analysis of interglacial trends in CO₂ over the last 650 Kyr (Fig. 5). After smoothing the record using a 5 Kyr running average, we define the beginning of an interglacial to be the local maximum in CO₂ following the upward crossing of a 255 ppm threshold. This definition yields appropriate dates of 10 Ka and 128 Ka for the beginning of the

last two interglacial periods and has the advantage of avoiding uncertainties in the relative timing of changes in ice volume and CO₂. The slope of the atmospheric CO₂ between the start of the interglacial and the subsequent 15 Kyr (or 10 Ky for the present interglacial) is determined using a least-squares fit. An average of globally-distributed benthic marine δ¹⁸O records (81) is used to estimate the magnitude of each deglaciation. Magnitudes are found by taking the δ¹⁸O difference between the local maximum and minimum bracketing each deglaciation after smoothing the δ¹⁸O record using a 5 Kyr running average. Trends in interglacial atmospheric CO₂ demonstrate a nearly linear relationship with the magnitude of deglaciation ($r^2 = 0.86$, $n = 6$, $p < 0.01$, Fig. 5). This suggests that the magnitude of deglaciation influences interglacial CO₂ trends, as anticipated from our glacio-volcano-CO₂ hypothesis (82). The present interglacial has a trend in CO₂ substantially more positive than predicted by the regression, suggesting the presence of an anomalous source of CO₂, possibly related to an early anthropogenic influence on atmospheric CO₂ (83).

We are able to make one further check of our analysis. The intercept of the regression relationship between CO₂ trends and deglacial magnitude is -8 ppm/Ky, which we interpret as the trend in interglacial CO₂ absent increased volcanic emissions. Neglecting feedbacks between volcanic CO₂ and other parts of the carbon system, we estimate the time history of non-volcanic atmospheric CO₂ by subtracting our mean estimate of the volcanic contribution to atmospheric CO₂ from the ice core observations of atmospheric CO₂ (Fig. 4e). Non-volcanic atmospheric CO₂ has a downward trend of -8 ppm/Ky during the period between 10 Ka and 6 Ka, in agreement with the downward trend predicted by the regression relationship. (We do not fit the trend over the more recent interval because of its anomalous behavior relative to other interglacials and the possibility of an anthropogenic influence.) Our reconstruction of volcanogenic atmospheric CO₂, bolstered by the strength of the regression relationship between the amplitude of deglaciation and the subsequent trends in atmospheric CO₂ during the late Pleistocene, indicates that volcanic emissions maintain high levels of atmospheric CO₂ during interglacials. In so much as high CO₂ inhibits deglaciation, we also expect that volcanic activity influences the duration of interglacials.

Discussion and conclusions

The analysis we have presented indicates a feedback between glacial cycles and subaerial volcanism. While there is both good observational evidence and theoretical support for the concept that deglacial unloading promotes volcanism, the climatic consequences of such increased volcanic activity are less clear on several counts: (1.) Primary CO₂ contents at both convergent and divergent margin magmas are insufficiently constrained. (2.) The relationship between total magma production rates and CO₂ emissions is not well understood. Much of the CO₂ loss must occur at depth during magma ascent and be added passively to the atmosphere rather than through eruption. (3.) We have not considered changes in rates of weathering, even though these are also expected to respond to variations in climate and glaciation. Finally, (4.) the rate of equilibration and partition of CO₂ between the atmosphere, ocean, biosphere, sediments, and solid earth is poorly constrained.

There is also a question regarding the relative importance of the competing volcanic influences on climate associated with atmospheric aerosol loading (2, 18, 84) and CO₂ emissions. Consider the case of the Mount Pinatubo eruption in 1991, which was well monitored and appears to be the second largest eruption within the last century. It injected about 17 Mt of SO₂ into the atmosphere and had a peak radiative cooling effect of 4W/m² at the surface, causing surface temperatures to cool by about 0.5°C (2). The aerosol cooling effect diminished with an e-folding time scale of approximately one year. By comparison, we estimate volcanism contributes ~40 ppm to the early interglacial atmosphere, causing an increase in radiative forcing of 1 W/m² (85). In this rough view, volcanic CO₂ forcing is equal in magnitude but opposite in sign to the aerosol effect of a Mount Pinatubo eruption every ~4 years. The competing influences of volcanic CO₂ and aerosol emissions is like the case of the tortoise and the hare: a persistent flux of CO₂ combined with a long atmospheric residence may make volcanic CO₂ emissions a powerful climate driver at glacial time scales. It is also possible that both cooling and warming effects had significance for the last deglaciation. Perhaps the large increase in volcanism near 12 Ka is associated with an increase in aerosol loading sufficient to drive some regions into a short-term resumption of glacial like conditions, i.e. the Younger Dryas. Climate may then have shifted back toward more interglacial-like conditions after a couple thousand years because of the continued increases in atmospheric

CO₂.

A balance appears to exist between emissions of CO₂ from volcanoes and uptake by weathering at hundred-thousand year and longer time scales (3). At shorter time scales, however, we suggest that deglacially induced anomalies in volcanic activity cause imbalances in the atmospheric carbon budget which accumulate through deglaciations and persist into interglacials. Volcanic emissions are often dismissed as too small to matter on glacial time scales, but the factor of two to five changes in activity that we document persist for thousands of years and are capable of increasing atmospheric concentrations by 20 to 80 ppm. While multiple other mechanisms must contribute to glacial/interglacial CO₂ variability (1, 71), the volcanic mechanism is notable for its coincidence with the observed secondary deglacial rise of atmospheric CO₂ (86). Thus, the deglacial rise and interglacial excess of CO₂ can, in part, be understood as a feedback induced by the deglaciation itself and mediated by volcanic activity. By similar logic, the glacial drawdown in CO₂ may partly owe to a deficit in volcanic emissions relative to CO₂ drawdown by weathering and other processes. All this suggests that the Earth system is deeply coupled. We expect interactions between the Earth's interior, surface, and atmosphere to amplify and modify the cycling between glacial and interglacial climates, so long as the climate and continental configuration engender co-location of volcanoes and ice. Finally, we estimate that volcanoes emit an excess 0.1 to 0.5 Gt of CO₂ during deglaciation. Humans presently emit ~30 Gt of CO₂ per year. If volcanic emissions influence the course of glacial/interglacial climates, it gives us pause that the accumulated volcanic CO₂ emissions during ~10,000 years of deglaciation would, at current rates, be replicated by only a century of anthropogenic emissions.

Acknowledgments We are grateful for the comments provided by R. Alley, C. Bacon, W. Broecker, G. Denton, T. Hughes, Peter Molnar, D. Schrag, D. Sigman, P. Wallace, and C. Wunsch, as well as for the guidance regarding marine carbonate chemistry from J. Higgins, D. Schrag, and D. Sigman. This work was supported by the National Science Foundation.

References and Notes

1. Broecker, W. S. & Peng, T. H. *Tracers in the sea* (Lamont-Doherty Earth Observatory of Columbia University, 1982).
2. Hansen, J., Laci, A., Ruedy, R. & Sato, M. Potential climate impact of Mount Pinatubo eruption. *Geophysical Research Letters* **19**, 215–218 (1992).
3. Walker, J., Hays, P. & Kasting, J. A negative feedback mechanism for the long-term stabilization of Earth's surface temperature. *J. of Geophysical Research* **86**, 9776–9782 (1981).
4. Grove, E. Deglaciation — a possible triggering mechanism for recent volcanism. In Gonzales, F. (ed.) *Proceedings of Symposium on Andean and Antarctic volcanology problems*, 88–97 (IAVCEI Proc., 1976).
5. Johnson, M. & Mauk, F. Earth tides and the triggering of eruptions from Mount Stromboli. *Nature* **239**, 266–267 (1972).
6. Hamilton, W. Tidal cycles of volcanic eruptions: Fortnightly to 19 yearly periods. *J. Geophys. Res.* **78**, 3356–3375 (1973).
7. Dzurisin, D. Influence of fortnightly earth tides at Kilauea volcano, Hawaii. *Geophys. Res. Lett.* **7**, 925–928 (1980).
8. Sparks, R. Triggering of volcanic eruptions by earth tides. *Nature* **290**, 448 (1981).
9. Neuberg, J. External modulation of volcanic activity. *Geophys. J. Int.* **142** (2000).

10. Saar, M. & Manga, M. Seismicity induced by seasonal ground-water recharge at Mt. Hood, Oregon. *Earth Planet. Sci. Lett.* **187**, 367–379 (2003).
11. Mason, B., Pyle, D., Dade, W. & Jupp, T. Seasonality of volcanic eruptions. *J. Geophys. Res.* **109** (2004).
12. Rampino, M., Self, S. & Fairbridge, R. Can rapid climate change cause volcanic eruptions? *Science* **206**, 826–828 (1979).
13. Hall, K. Rapid deglaciation as an initiator of volcanic activity: An hypothesis. *Earth Surf. Processes Landforms* **206**, 45–51 (1982).
14. Sigvaldson, G., Annertz, K. & Nilsson, M. Effect of glacier loading/deloading on volcanism: Postglacial volcanic eruption rate of the Dyngjufjoll area, central Iceland. *Bull. Volcanol.* **54**, 385–392 (1992).
15. Nakada, M. & Yokose, H. Ice age as a trigger of active Quaternary volcanism and tectonism. *Tectonophysics* **212**, 321–329 (1992).
16. Paterne, M. & Guichard, F. Triggering of volcanic pulses in the Campanian area, South Italy by periodic deep magma influx. *J. Geophys. Res.* **98**, 1861–1873 (1993).
17. Jull, M. & Mckenzie, D. The effect of deglaciation on mantle melting beneath Iceland. *J. Geophys. Res.* **101**, 21815–21828 (1996).
18. Zielinski, G. Use of paleo-records in determining variability within the volcanism-climate system. *Quaternary Science Reviews* **19**, 417–438 (2000).
19. Jellinik, A., Manga, M. & Saar, M. Did melting glaciers cause volcanic eruptions in eastern California? Probing the mechanics of dike formation. *J. of Geophys. Res.* **109** (2004).
20. Zielinski, G. *et al.* Volcanic aerosol records and tephrochronology of the Summit, Greenland, ice cores. *J. Geophys. Res.* **102** (1997).

21. Maclennan, J., Jull, M., McKenzie, D., Slater, L. & Grönvold, K. The link between volcanism and deglaciation in Iceland. *Geochem. Geophys. Geosyst* **3**, 1062 (2002).
22. Nowell, D., Jones, C. & Pyle, D. Episodic quaternary volcanism in France and Germany. *J. Quatern. Sci.* **21**, 645–675 (2006).
23. Glazner, A., Manley, C., Marron, J. & Rojstaczer, S. Fire or ice: Anticorrelation of volcanism and glaciation in California over the past 800,000 years. *Geophys. Res. Lett.* **26**, 1759–1792 (1999).
24. Bacon, C. & Lanphere, M. Eruptive history and geochronology of Mount Mazama and the Crater Lake region, Oregon. *GSA Bulletin* **118(11-12)**, 1331–1359 (2006).
25. Best, J. Sedimentology and event timing of a catastrophic volcanoclastic mass-flow, Volcan Hudson, southern Chile. *Bull. Volcanol.* **54**, 299–318 (1992).
26. Gardeweg, M., Sparks, R. & Mathews, S. Evolution of Lascar volcano, northern Chile. *J. Geol. Soc. Lond.* **155**, 89–104 (1998).
27. Bryson, R. U., Bryson, R. A. & Ruter, A. A calibrated radiocarbon database of late quaternary volcanic eruptions. *eEarth Discuss* **1**, 123–134 (2006).
28. Simkin, T. & Siebert, L. *Volcanoes of the World, 2nd ed.* (Geoscience, Tucson, Ariz., 1994).
29. Siebert, L. & Simkin, T. Volcanoes of the world: an illustrated catalog of Holocene volcanoes and their eruptions. *Smithsonian Institution, Global Volcanism Program, Digital Information Series, GVP-3* (2002).
30. The date of most volcanic events is uncertain (29), and we use a probability distribution to describe when each event occurred. We use the reported calendar age uncertainties for each event, or in the case of radiocarbon, we propagate the uncertainty through the calibration curve. Radiocarbon dates and their uncertainties are adjusted to calendar ages using an approach based on the CALIB program (Stuiver, Reimer, and Reimer, <http://calib.qub.ac.uk/calib>). Ages

without a reported uncertainty are assumed to have a normal probability distribution with a standard deviation of ten percent of the age, which is large relative to most dating uncertainties. In this manner, the dataset of 5352 events and their uncertain ages are transformed into an equal number of probability distribution spanning the interval from 40,000 years ago to the present (Fig. 1).

31. Denton, G. & Hughes, T. *The Last Great Ice Sheets* (Wiley-Interscience, 1981).
32. Grosswald, M. Late-Weichselian ice sheets in Arctic and Pacific Siberia. *Quaternary International* **45**, 3–18 (1998).
33. Yu, Z., Walker, K., Evenson, E. & Hajdas, I. Late glacial and early Holocene climate oscillations in the Matanuska Valley, south-central Alaska. *Quaternary Science Reviews* **27**, 148–161 (2008).
34. Dyke, S. An outline of North American deglaciation with emphasis on central and northern Canada. In *Quaternary Glaciations: Extent and Chronology*, 400 (Elsevier, 2004).
35. McCulloch, R. *et al.* Climatic inferences from glacial and palaeoecological evidence at the last glacial termination, southern South America. *Journal of Quaternary Science* **15**, 409–417 (2000).
36. Kalnay, E. *et al.* The NCEP/NCAR 40-Year Reanalysis Project. *Bulletin of the American Meteorological Society* **77**, 437–471 (1996).
37. Ice mass balance is calculated by taking the difference between net precipitation, taken from NCEP reanalysis (36), and net ablation. Ablation is calculated using daily average two-meter temperatures, also from NCEP, and a positive degree approach where daily average temperatures that exceed freezing are converted into 0.15 mm/(day °C) of melt. All melt is assumed to run off.

38. Cogely, J. G. Global hydrographic data, release 2.3. *Trent Technical Note 2003-1, Department of Geography, Trent University, Petersborough, Ontario, Canada*. Data are available at <http://www.trentu.ca/academic/geography/glaciology/glgghy.htm> (2003).
39. A bias against observing volcanic eruptions is expected to be largest in glaciated regions because processes such as ash emplacement on snow or tephra scoured by ice would tend to destroy evidence of the eruption. A larger observational bias in glaciated regions would lead to an underestimate of the global increase in volcanism during deglaciation, suggesting that our results may be an underestimate.
40. The statistical significance of the increase in global volcanism is estimated using a Monte Carlo approach wherein we compute changes in global volcanic activity after randomly assigning volcanic events to the glaciated and unglaciated groups. 99% of all the randomized trials lie within a region between half and twice modern eruption rates for any given year, indicating that the observed increase in global volcanic activity during deglaciation, at more than double modern rates, is highly significant.
41. Zielinski, G., Mayewski, P., Meeker, L., Whitlow, S. & Twickler, M. A 110,000-Yr Record of Explosive Volcanism from the GISP2 (Greenland) Ice Core. *Quaternary Research* **45**, 109–118 (1996).
42. Walcott, R. Past sea levels, eustasy and deformation of the Earth. *Quat. Res.* **2**, 1–14 (1972).
43. Wallmann, P., Mahood, G. & Pollard, D. Mechanical models for correlation of ring fracture eruptions at Pantelleria, Strait of Sicily, with glacial sea level drawdown. *Bull. Volcanol.* **50**, 327–339 (1988).
44. McGuire, W. *et al.* Correlation between rate of sea level change and frequency of explosive volcanism in the Mediterranean. *Nature* **389**, 473–476 (1997).
45. Jupp, T., Pyle, D., Mason, B. & Dade, W. A statistical model for the timing of earthquakes and volcanic eruptions influenced by periodic processes. *J. Geophys. Res.* **109(B02206)** (2004).

46. Reymer, A. & Schubert, G. Phanerozoic addition rates to the continental crust and crustal growth. *Tectonics* **3**, 63–77 (1984).
47. Dimilanta, C., Taira, A., Tokuyama, H., Yumul, G. & Mochizuki, K. New rates of western pacific island arc magmatism from seismic and gravity data. *Earth and Planetary Science Letters* **202**, 105–115 (2002).
48. Crisp, J. Rates of magma emplacement and volcanic output. *J. volcanol. geotherm. res.* **20**, 177–211 (1984).
49. Carmichael, I. The andesite aqueduct: perspectives on the evolution of intermediate magmatism in west-central (105–99° W) Mexico. *Contributions to Mineralogy and Petrology* **143**, 641–663 (2002).
50. Wallace, P. Volatiles in subduction zone magmas: concentrations and fluxes based on melt inclusion and volcanic gas data. *Journal of Volcanology and Geothermal Research* **140**, 217–240 (2005).
51. Saal, A., Hauri, E., Langmuir, C. & Perfit, M. Vapour undersaturation in primitive mid-ocean-ridge basalt and the volatile content of Earth’s upper mantle. *Nature* **419**, 451–455 (2002).
52. Cartigny, P., Pineau, F., Aubaud, C. & Javoy, M. Towards a consistent mantle carbon flux estimate: Insights from volatile systematics (H₂O/Ce, δ D, CO₂/Nb) in the North Atlantic mantle (14 N and 34 N). *Earth and Planetary Science Letters* (2007).
53. Marty, B. & Tolstikhin, I. CO₂ fluxes from mid-ocean ridges, arcs and plumes. *Chemical Geology* **145**, 233–248 (1998).
54. Fischer, T., Giggenbach, W., Sano, Y. & Williams, S. Fluxes and sources of volatiles discharged from Kudryavy, a subduction zone volcano, Kurile Islands. *Earth and Planetary Science Letters* **160**, 81–96 (1998).

55. Hilton, D., Fischer, T. & Marty, B. Nobel gases and volatile recycling at subduction zones. In Prcelli, D., Ballentine, C. & Wieler, R. (eds.) *Noble Gases in Geochemistry and Cosmochemistry*, vol. 47, 319–370 (Review in Mineralogy and Geochemistry, 2002).
56. Allard, P., Carbonnelle, J., Dajlevic, D., Le Bronce, J. & Morel, P. Eruptive and diffuse emissions of CO₂ from Mount Etna. *Nature* **351**, 387–391 (1991).
57. Allard, P., Carbonnelle, J., Metrich, N., Loyer, H. & Zettwoog, P. Sulphur output and magma degassing budget of Stromboli volcano. *Nature* **368**, 326–330 (1994).
58. Williams, S., Schaefer, S. *et al.* Global carbon dioxide emission to the atmosphere by volcanoes. *Geochimica et Cosmochimica Acta* **56**, 1765–1770 (1992).
59. Goff, F. *et al.* Passive infrared remote sensing evidence for large, intermittent CO₂ emissions at Popocatépetl volcano, Mexico. *Chemical Geology* **177**, 133–156 (2001).
60. Varekamp, J., Kreulen, R., Poorter, R. & Van Bergen, M. Carbon sources in arc volcanism, with implications for the carbon cycle. *Terra Nova* **4**, 363–373 (1992).
61. Sano, Y. & Marty, B. Origin of carbon in fumarolic gas from island arcs. *Chem. Geol.* **119**, 265–274 (1995).
62. Sano, Y. & Williams, S. Fluxes of mantle and subducted carbon along convergent plate boundaries. *Geophys. Res. Lett.* **23**, 2749–2752 (1996).
63. Gorman, P., Kerrick, D. & Connolly, J. Modeling open system metamorphic decarbonation of subducting slabs. *Geochem. Geophys. Geosyst* **7** (2006).
64. Khesgi, H. Ocean carbon sink duration under stabilization of atmospheric CO₂: A 1,000-year timescale. *Geophysical Research Letters* **31** (2004).
65. Archer, D. Fate of fossil fuel CO₂ in geologic time. *J. of Geophys. Res.* **110(C09S05)** (2005).

66. Montenegro, ., Brovkin, V., Eby, M., Archer, D. & Weaver, A. Long term fate of anthropogenic carbon. *Geophys. Res. Lett.* **L19707** (2007).
67. Wunsch, C. & Heimbach, P. How long to oceanic tracer and proxy equilibrium? *Quaternary Science Reviews* (in press).
68. Monnin, E. *et al.* Atmospheric CO₂ Concentrations over the Last Glacial Termination (2001).
69. Smith, H. J., Fischer, H., Wahlen, M., Mastroianni, D. & Deck, B. Dual modes of the carbon cycle since the last glacial maximum. *Nature* **400**, 248–250 (1999).
70. Indermühle, A., Monnin, E., Stauffer, B., Stocker, T. & Wahlen, M. Atmospheric CO₂ concentration from 60 to 20 kyr BP from the Taylor Dome ice core, Antarctica. *Geophys. Res. Lett* **27**, 735–738 (2000).
71. Köhler, P. & Fishcer, H. Simulating low frequency changes in atmospheric CO₂ during the last 740 000 years. *Climate of the Past* **2**, 57–78 (2006).
72. Schrag, D., Hampt, G. & Murray, D. Pore fluid constraints on the temperature and oxygen isotopic composition of the glacial ocean. *Science* **272**, 1930–1932 (1996).
73. Farrell, J. & Prell, W. Climatic change and CaCO₃ preservation: An 800,000 year bathymetric reconstruction from the central equatorial Pacific Ocean. *Paleoceanography* **4**, 447–466 (1989).
74. Thunell, R., Qingmin, M., Calvert, S. & Pedersen, T. Glacial-Holocene biogenic sedimentation patterns in the South China Sea: Productivity variations and surface water pCO₂. *Paleoceanography* **7**, 143–162 (1992).
75. Curry, W. B., Duplessy, J.-C., Labeyrie, L. D. & Shackleton, N. J. Changes in the distribution of $\delta^{13}\text{C}$ of deepwater ΣCO_2 between the last glaciation and the Holocene. *Paleoceanography* **3**, 317–341 (1988).

76. Shaw, A., Hilton, D., Fishcer, T., Walker, J. & Alvarado, G. Contrasting He-C relationships in Nicaragua and Costa Rica: insights into C cycling through subduction zones. *Earth Planet. Sci. Lett.* **214**, 499–513 (2003).
77. de Leeuw, G., Hilton, D., Fischer, T. & Walker, J. The He–CO₂ isotope and relative abundance characteristics of geothermal fluids in El Salvador and Honduras: New constraints on volatile mass balance of the Central American Volcanic Arc. *Earth and Planetary Science Letters* **258**, 132–146 (2007).
78. Vecsei, A. & Berger, W. Increase of atmospheric CO₂ during deglaciation: Constraints on the coral reef hypothesis from patterns of deposition. *Global Biogeochemical Cycles* **18** (2004).
79. Petit, J. *et al.* Climate and atmospheric history of the past 420,000 years from the Vostok ice core, Antarctica. *Nature* **399**, 429–436 (1999).
80. Siegenthaler, U. *et al.* Stable carbon cycle-climate relationship during the late Pleistocene. *Science* **310**, 1313–1317 (2005).
81. Huybers, P. Glacial variability over the last 2Ma: an extended depth-derived agemodel, continuous obliquity pacing, and the Pleistocene progression. *Quat. Sci. Rev.* **26**, 37–55 (2007).
82. It might also be expected for trends in atmospheric CO₂ to depend on the magnitude of CO₂ concentration, but the CO₂ concentration at the beginning of a deglaciation and the subsequent trends have no obvious relationship ($r^2 = 0.0$). This suggests that early interglacial trends in CO₂ depend more on the past history of deglaciation than on the immediate atmospheric composition.
83. Ruddiman, W. F. Orbital insolation, ice volume, and greenhouse gases. *Quaternary Science Reviews* **22**, 1597–1622 (2003).
84. Rampino, M. & Self, S. Volcanic winter and accelerated glaciation following the Toba super-eruption. *Nature* **359**, 50–52 (1992).

85. Radiative forcing is estimated as $F = 5.35 \ln((C_o + C)/C_o)$ (87) where we take C_o as 200 ppm, somewhat above the glacial value.
86. The well-documented co-variability between Antarctic temperature and CO_2 has been interpreted as evidence for Southern Ocean control over atmospheric CO_2 concentrations (68), but it could equally be the case that variations in atmospheric CO_2 , accompanied by sea ice and other positive feedbacks, largely controls Antarctic temperature.
87. Houghton, J. *et al.* (eds.) *Climate Change 2001: The Scientific Basis. Contribution of Working Group I to the Third Assessment Report of the Intergovernmental Panel on Climate Change* (Cambridge University Press, 2001).
88. Fairbanks, R. & Peltier, W. Global glacial ice volume and Last Glacial Maximum duration from an extended barbados sea level record. *Quaternary Science Reviews* **25**, 3322–3337 (2006).
89. Monnin, E. *et al.* Evidence for substantial accumulation rate variability in Antarctica during the Holocene, through synchronization of CO_2 in the Taylor Dome, Dome C and DML ice cores. *Earth and Planetary Science Letters* **224**, 45–54 (2004).

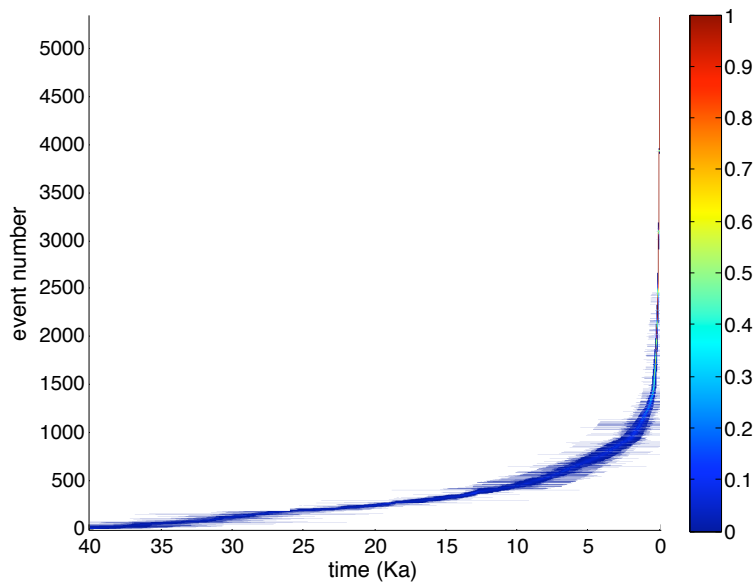


Fig. 1: The timing of volcanic events in our combined database. Shading indicates the probability that a volcanic event occurred within each 50 year interval between 40 Ka and the present. Events are listed in order of the expected value of their age. Note the observational bias toward recent years; $\sim 80\%$ of the events occur within the last 1000 years.

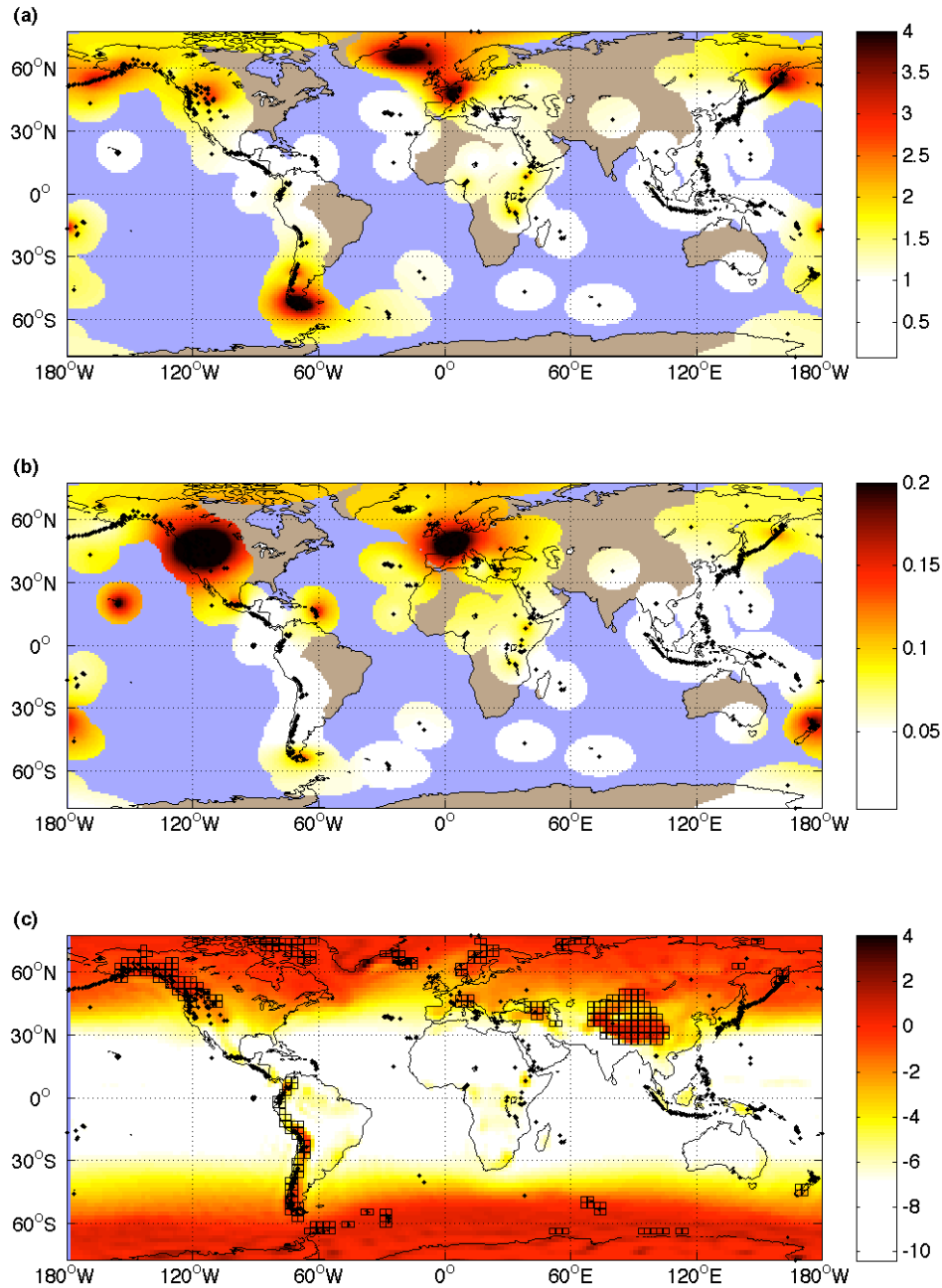


Fig. 2: Volcanic activity maps. **(a)** The ratio of deglacial (17 Ka and 7 Ka) to glacial (40 Ka and 20 Ka) volcanic activity. Activity ratios (white-red shading) are only shown in regions within a 10° radius of a volcano (black dots). **(b)** Similar to (a) but the ratio between deglacial (17 Ka and 7 Ka) and late Holocene (5 Ka to the present) activity. Note the difference in scale between (a) and (b) which reflects the observational bias towards fewer eruptions identified in the past. **(c)** The modern ice mass balance estimated from NCEP reanalysis (36) (shading in m/yr) is used as a proxy for the magnitude of deglaciation. The mass balance is almost everywhere negative because the resolution of the NCEP smooths the highest topographic features and spreads out regions of concentrated rainfall. Nonetheless, regions presently containing glaciers (38) (indicated by 3° × 3° black grid boxes) coincide with the least negative mass balance values.

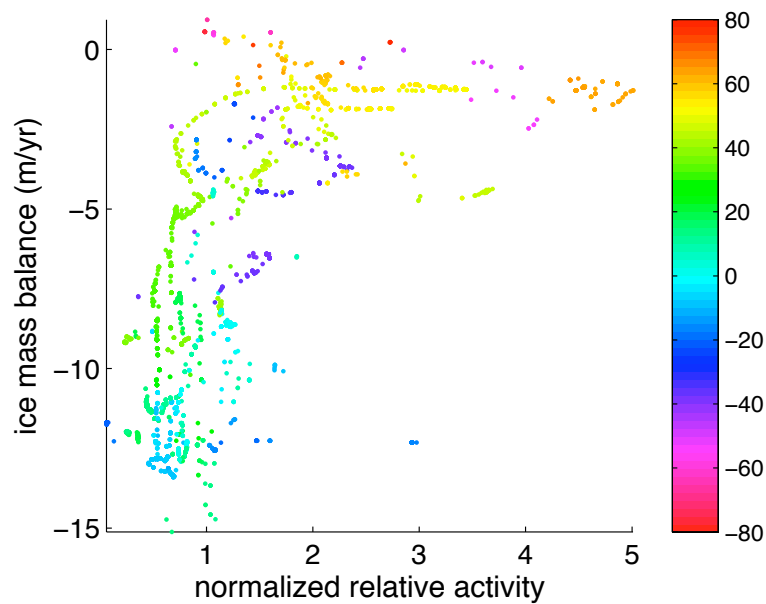


Fig. 3: The deglacial activity ratio at each volcano (Fig. 2a,b) is plotted against the proxy for the magnitude of the deglaciation (Fig. 2c). Activity ratios are taken with respect to both glacial (Fig. 2a) and inter-glacial (Fig. 2b) values and, after normalized to unit variance, are averaged together. Deglacial activities are greater in regions which underwent greater deglaciation. Likewise, volcanoes at higher latitudes (latitude is indicated by the shading) were generally more active during the last deglaciation.

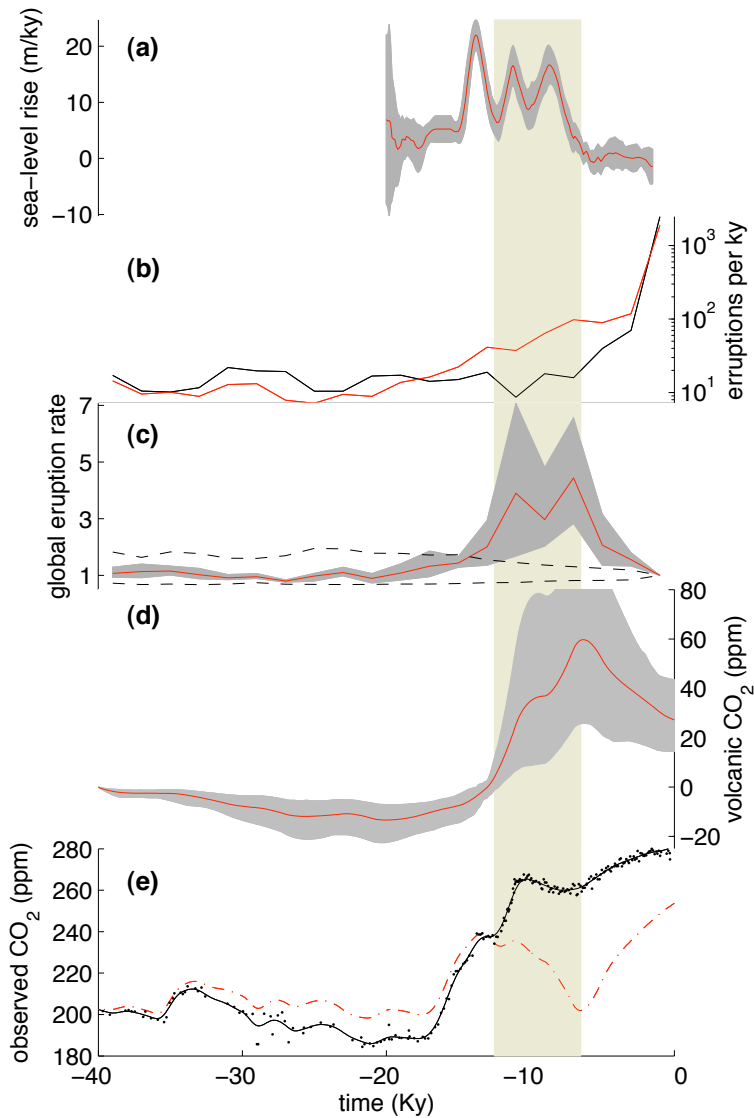


Fig. 4: Sequence of events from the last glacial to the present. **(a)** The rate of change in sea level estimated from coral records (88) along with a Monte Carlo derived estimate of the 90% confidence interval (gray shading). **(b)** The number of volcanic events per Kyr for glaciated (red) and unglaciated (black) volcanoes, combined from two datasets (27, 29). Note that the y-axis is logarithmic. **(c)** Estimated global volcanic activity (both glaciated and unglaciated, red line). Dashed lines indicate the 99% interval for the null-hypothesis of no systematic difference between glaciated and unglaciated events, which our deglacial estimates greatly exceed. **(d)** The contribution to atmospheric CO₂ from volcanic activity (red line). Quantities indicated by solid lines and gray shading in b, c, and d are the averages and 90% confidence intervals derived from a 10,000 member ensemble of model runs (see text). **(e)** CO₂ concentrations from Dome C (68) and Taylor Dome (69, 70), placed on a consistent timescale (89) (black dots), and a smoothed version using a 2 Kyr window (black line). Also shown is the residual atmospheric CO₂ after removal of the volcanic contribution (red dash-dot line). The vertical shaded bar indicates the time period between 12 Ka and 7 Ka.

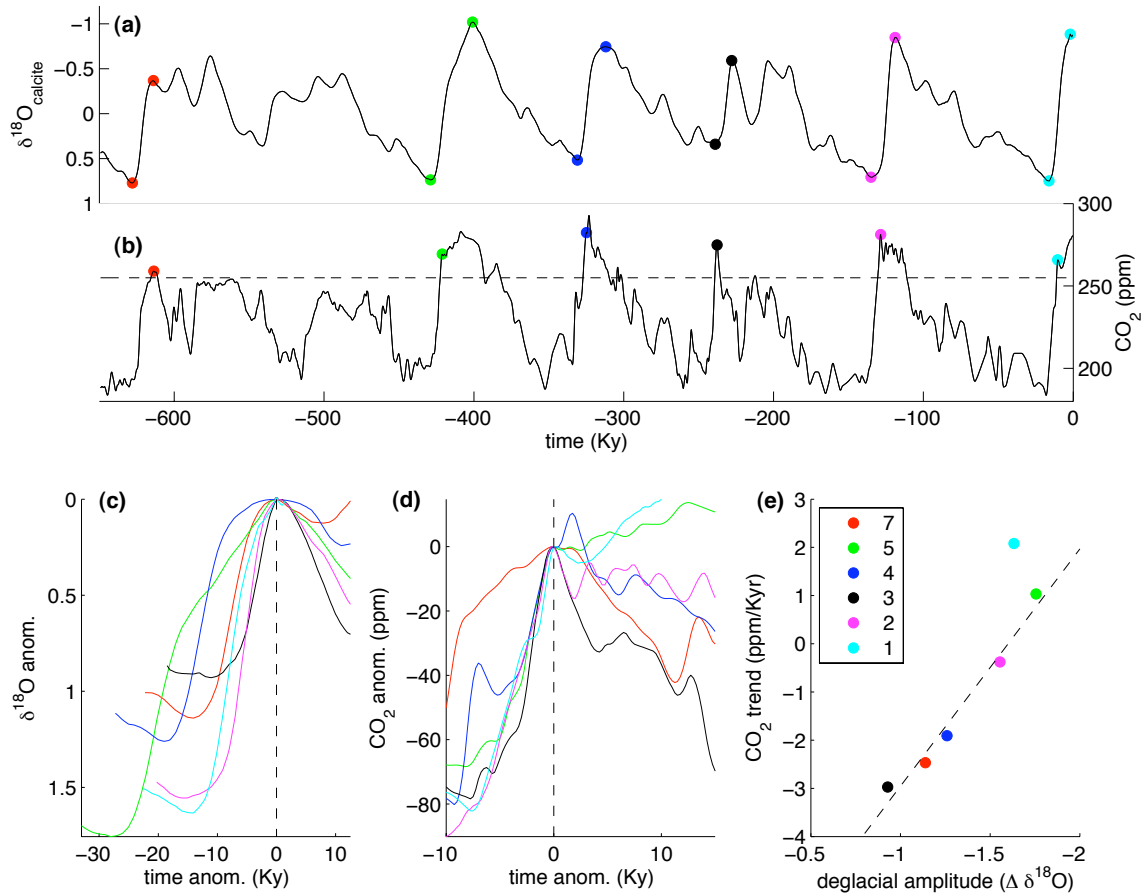


Fig. 5: A simple relationship exists between the magnitude of deglaciation and interglacial trends in atmospheric CO_2 during the late Pleistocene. **(a)** An average of many benthic marine $\delta^{18}\text{O}_{\text{calcite}}$ records (81) is used as a proxy for changes in ice volume. Dots indicate the local minimum and maximum bracketing each termination. Values are departures from the mean, and the y-axis is reversed. **(b)** The combined atmospheric CO_2 record from Vostok (79) and EPICA Dome C (80). The beginning of interglacials are identified as the first local maximum following an upward crossing of a 255 ppm threshold (dots). **(c)** Detail of each glacial termination as recorded in the benthic $\delta^{18}\text{O}$ record. Time and amplitude are expressed as departures from the local minimum following deglaciation. Colors indicate the termination number with one being the most recent. **(d)** Deglacial and interglacial CO_2 values indicated as departures from the local maximum following deglaciation. **(e)** Amplitude of the deglaciation plotted against the trend in interglacial CO_2 values. CO_2 trends are fit over the 15 Kyr subsequent to deglaciation or, for the Holocene, the 10 Kyr available to us. Termination six is excluded because its interglacial CO_2 values are too low. The anomalous behavior of termination one may reflect an anthropogenic influence.